



## Plane Wave Diffraction by a Thin Material Strip: the Case of E Polarization

Takashi Nagasaka<sup>\*(1)</sup> and Kazuya Kobayashi<sup>(1)</sup>

(1) Department of Electrical, Electronic, and Communication Engineering, Chuo University  
1-13-27 Kasuga, Bunkyo-ku, Tokyo 112-8551, Japan

### Abstract

The diffraction by a thin material strip is analyzed for the E-polarized plane wave incidence using the Wiener-Hopf technique together with approximate boundary conditions. An asymptotic solution is obtained for the case where the thickness and the width of the strip are small and large compared with the wavelength, respectively. The scattered field is evaluated asymptotically based on the saddle point method and a far field expression is derived. Scattering characteristics are discussed in detail via numerical results of the radar cross section.

### 1. Introduction

The analysis of the scattering by material strips is an important subject in electromagnetic theory and radar cross section (RCS) studies. Volakis [1] analyzed the H-polarized plane wave diffraction by a thin material strip using the dual integral equation approach and the extended spectral ray method together with approximate boundary conditions [2]. In his paper [1], Volakis first solved rigorously the diffraction problem involving a single material half-plane, and subsequently obtained a high-frequency solution to the original strip problem by superposing the singly diffracted fields from the two independent half-planes and the doubly/triply diffracted fields from the edges of the two half-planes. Therefore his analysis is not rigorous from the viewpoint of boundary value problems, and may not be applicable unless the strip width is relatively large compared with the wavelength. This problem has been solved more recently by Shapoval *et al.* [3] by using the generalized boundary conditions and the singular integral equation.

In [4], we have reconsidered Volakis's problem [1] and obtained a more rigorous, high-frequency solution using the Wiener-Hopf technique [5] together with approximate boundary conditions. In particular, it has been verified that our solution does incorporate the multiple diffraction effect between the edges of the strip and is valid for the strip width not too small compared with the wavelength. In this paper, we shall consider the same geometry for the material strip, and analyze the E-polarized plane wave diffraction via a method similar to that developed in our previous paper [4].

Introducing the Fourier transform of the scattered field and applying approximate boundary conditions in the

transform domain, the problem is formulated in terms of the Wiener-Hopf equations, which are solved exactly via the factorization and decomposition procedure. However, the solution is formal in the sense that branch-cut integrals with unknown integrands are involved. By employing a rigorous asymptotic method developed by the second-named author [6] together with the special function introduced in our previous paper [4], we shall derive a high-frequency solution of the Wiener-Hopf equations, which is valid for the strip width greater than about the incident wavelength. The scattered field in the real space is evaluated asymptotically by taking the Fourier inverse of the solution in the transform domain and applying the saddle point method of integration. Numerical examples of the RCS are presented for various physical parameters and far field scattering characteristics of the strip are discussed. Some comparisons with other methods are also provided and the validity of our approach is discussed.

The time factor is assumed to be  $e^{-i\omega t}$  and suppressed throughout this paper.

### 2. Formulation of the Problem

We consider the diffraction of an E-polarized plane wave by a thin material strip as shown in Figure 1, where the relative permittivity and permeability of the strip are denoted by  $\epsilon_r$  and  $\mu_r$ , respectively. Let the total electric field  $\phi^t(x, z) [\equiv E_y^t(x, z)]$  be

$$\phi^t(x, z) = \phi^i(x, z) + \phi(x, z), \quad (1)$$

where  $\phi^i(x, z)$  is the incident field given by

$$\phi^i(x, z) = e^{-ik(x \sin \theta_0 + z \cos \theta_0)}, \quad 0 < \theta_0 < \pi/2 \quad (2)$$

with  $k [= \omega(\epsilon_0 \mu_0)^{1/2}]$  being the free-space wavenumber. The term  $\phi(x, z)$  is the unknown scattered field and satisfies the two-dimensional Helmholtz equation.

If the strip thickness  $b$  is small compared with the wavelength, the material strip is approximately replaced by a strip of zero thickness satisfying the second-order impedance boundary conditions [2]. On the strip surface, the total electromagnetic fields satisfy the approximate boundary conditions as given by

$$\begin{aligned} & \left[ \frac{1}{R_e} + \frac{1}{R_m} \left( 1 + \frac{1}{k^2} \frac{\partial^2}{\partial x^2} \right) \right] [E_y^t(+0, z) + E_y^t(-0, z)] \\ & = -2[H_z^t(+0, z) - H_z^t(-0, z)], \end{aligned} \quad (3)$$

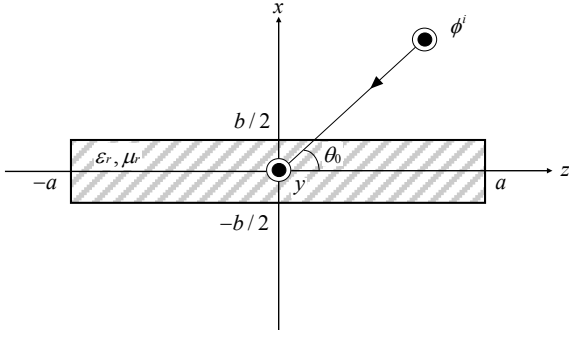


Figure 1. Geometry of the problem.

$$\begin{aligned} & [H'_z(+0, z) + H'_z(-0, z)] \\ & = -2R_m[E'_y(+0, z) - E'_y(-0, z)], \end{aligned} \quad (4)$$

where

$$\left. \begin{aligned} R_e &= iZ_0/[kb(\epsilon_r - 1)], R_m = iY_0/[kb(\mu_r - 1)], \\ \tilde{R}_m &= iZ_0\mu_r/[kb(\mu_r - 1)] \end{aligned} \right\} \quad (5)$$

with  $Z_0$  and  $Y_0$  being the intrinsic impedance and admittance of free space, respectively. In the following, we shall assume that the medium is slightly lossy as in  $k = k_1 + ik_2$  with  $0 < k_2 \ll k_1$ .

Let us define the Fourier transform of the scattered field  $\phi(x, z)$  with respect to  $z$  as

$$\Phi(x, \alpha) = (2\pi)^{-1/2} \int_{-\infty}^{\infty} \phi(x, z) e^{i\alpha z} dz, \quad (6)$$

where  $\alpha = \sigma + i\tau$ . Then we see with the aid of the radiation condition that  $\Phi(x, \alpha)$  is regular in the strip  $|\tau| < k_2 \cos \theta_0$  of the complex  $\alpha$ -plane. Introducing the Fourier integrals as

$$\Phi_{\pm}(x, \alpha) = \pm(2\pi)^{-1/2} \int_{\pm a}^{\pm\infty} \phi(x, z) e^{i\alpha(z \mp a)} dz, \quad (7)$$

it is found that  $\Phi_{\pm}(x, \alpha)$  are regular in  $\tau \gtrless \mp k_2 \cos \theta_0$ .

Taking the Fourier transform of the Helmholtz equation and solving the resultant equation, we find that

$$\Phi(x, \alpha) = \hat{\Phi}(\alpha) e^{-\gamma|x|}, \quad (8)$$

where  $\gamma = (\alpha^2 - k^2)^{1/2}$  with  $\text{Re } \gamma > 0$ , and

$$\begin{aligned} \hat{\Phi}(\alpha) &= -ikZ_0[e^{-i\alpha a}U_-(\alpha) + e^{i\alpha a}U_+(\alpha)]/[2\gamma M(\alpha)] \\ & \mp [e^{-i\alpha a}V_-(\alpha) + e^{i\alpha a}V_+(\alpha)]/K(\alpha), \quad x \gtrless 0 \end{aligned} \quad (9)$$

with

$$K(\alpha) = \gamma - 2ikZ_0R_m, \quad (10)$$

$$M(\alpha) = 1 - \frac{ikZ_0}{2\gamma} \left[ \frac{1}{R_e} + \frac{1}{\tilde{R}_m} \left( 1 + \frac{\gamma^2}{k^2} \right) \right], \quad (11)$$

$$V_{(\pm)}(\alpha) = \Phi'_{\pm}(\alpha) \mp \frac{B_{1,2}}{\alpha - k \cos \theta_0}, \quad (12)$$

$$U_{(\pm)}(\alpha) = \tilde{\Phi}_{\pm}(\alpha) \mp \frac{A_{1,2}}{\alpha - k \cos \theta_0}, \quad (13)$$

$$\Phi'_{\pm}(\alpha) = \frac{d\Phi_{\pm}(0, \alpha)}{dx}, \quad (14)$$

$$\tilde{\Phi}_{\pm}(\alpha) = \left( \frac{1}{R_e} + \frac{1}{\tilde{R}_m} \right) \Phi_{\pm}(0, \alpha) + \frac{1}{\tilde{R}_m k^2} \frac{d^2 \Phi_{\pm}(0, \alpha)}{dx^2}, \quad (15)$$

$$B_{1,2} = -(2\pi)^{-1/2} k \sin \theta_0 e^{\mp ika \cos \theta_0}, \quad (16)$$

$$A_{1,2} = -(2\pi)^{-1/2} i \left( \frac{1}{R_e} + \frac{\cos^2 \theta_0}{\tilde{R}_m} \right) e^{\mp ika \cos \theta_0}. \quad (17)$$

Equation (8) is the scattered field representation in the Fourier transform domain. Using the boundary conditions, we obtain from (9) that

$$-K(\alpha)J_m(\alpha) = 2[e^{-i\alpha a}V_-(\alpha) + e^{i\alpha a}V_+(\alpha)], \quad (18)$$

$$M(\alpha)J_e(\alpha) = e^{-i\alpha a}U_-(\alpha) + e^{i\alpha a}U_+(\alpha), \quad (19)$$

where  $J_e(\alpha)$  and  $J_m(\alpha)$  denote the Fourier transforms of the unknown electric and magnetic surface currents on the strip, respectively, and are entire functions. Equations (18) and (19) are the Wiener-Hopf equations satisfied by the unknown spectral functions.

### 3. Exact Solution

The kernel functions  $M(\alpha)$  and  $K(\alpha)$  defined by (10) and (11) can be factorized as

$$K(\alpha) = K_+(\alpha)K_-(\alpha) = K_+(\alpha)K_+(-\alpha), \quad (20)$$

$$M(\alpha) = M_+(\alpha)M_-(\alpha) = M_+(\alpha)M_+(-\alpha), \quad (21)$$

where

$$K_{\pm}(\alpha) = (2kZ_0R_m)^{1/2} e^{-i\pi/4} N_{3\pm}(\alpha), \quad (22)$$

$$M_{\pm}(\alpha) = \left[ \frac{kZ_0}{2} \left( \frac{1}{R_e} + \frac{1}{\tilde{R}_m} \right) \right]^{1/2} \frac{N_{1\pm}(\alpha)N_{2\pm}(\alpha)}{(k \pm \alpha)^{1/2}} \quad (23)$$

with

$$\begin{aligned} N_{n\pm}(\alpha) &= (1 + \delta_n^{-1})^{1/2} \\ & \cdot \exp \left\{ -\frac{\delta_n}{\pi} \int_{\pi/2}^{\arccos(\pm\alpha/k)} \frac{t \cos t}{\sin^2 t - \delta_n^2} dt \right. \\ & \left. + \frac{1}{4} \ln \left[ 1 + \frac{\alpha^2}{k^2(\delta_n^2 - 1)} \right] \pm \ln[\delta_n + (\delta_n^2 - 1)^{1/2}] \right. \\ & \left. \cdot \frac{i}{2\pi} \ln \left[ \frac{ik(\delta_n^2 - 1)^{1/2} + \alpha}{ik(\delta_n^2 - 1)^{1/2} - \alpha} \right] \right\}, \quad n = 1, 2, 3, \end{aligned} \quad (24)$$

$$\begin{aligned} \delta_{1,2} &= -\frac{\tilde{R}_m}{Z_0} \left\{ 1 \pm \left[ 1 + \frac{Z_0^2}{\tilde{R}_m} \left( \frac{1}{R_e} + \frac{1}{\tilde{R}_m} \right) \right]^{1/2} \right\}, \\ \delta_3 &= 2Z_0R_m. \end{aligned} \quad (25)$$

We multiply both sides of (18) by  $e^{\pm i\alpha a} / K_{\mp}(\alpha)$  and apply the decomposition procedure with the aid of the edge condition. This leads to

$$\begin{aligned} V_{(\pm)}^{s,d}(\alpha) &= K_+(\alpha) \left[ -\frac{B_1}{K_+(k \cos \theta_0)(\alpha - k \cos \theta_0)} \right. \\ & \left. \mp \frac{B_2}{K_-(k \cos \theta_0)(\alpha + k \cos \theta_0)} \pm v_{s,d}(\alpha) \right], \end{aligned} \quad (26)$$

where

$$v_{s,d}(\alpha) = \frac{1}{\pi i} \int_k^{k+i\infty} \frac{e^{2i\beta a} (\beta - k)^{1/2}}{\beta + \alpha} V_{(\pm)}^{s,d}(\beta) T_{\pm}(\beta) d\beta, \quad (27)$$

$$V_{(+)}^{s,d}(\alpha) = V_{(+)}(\alpha) \pm V_{-}(-\alpha) \quad (28)$$

with

$$T_{+}(\beta) = \frac{(\beta + k)^{1/2} K_{+}(\beta)}{\beta^2 - k^2 + 4k^2 Z_0^2 R_m^2}. \quad (29)$$

Equation (26) is the exact solution to the Wiener-Hopf equation (18), but it is formal since the branch-cut integrals with the unknown integrands  $v_{s,d}(\alpha)$  are involved. Equation (19) can be solved in a similar manner.

#### 4. High-Frequency Asymptotic Solution

In order to eliminate the singularities of  $V_{(+)}^{s,d}(\alpha)$  in (26) at  $\alpha = k \cos \theta_0$ , we introduce the functions

$$\Phi_{+}^{s,d}(\alpha) = \Phi_{+}'(\alpha) \pm \Phi_{-}'(-\alpha). \quad (30)$$

Applying the asymptotic method [4] developed by the second-named author, we can obtain a high-frequency asymptotic expansion of (26) with the result that

$$\Phi_{+}^{s,d}(\alpha) \sim K_{+}(\alpha) \cdot \left[ \chi_{vs,vd}(\alpha) + C_{s,d} \sum_{n=0}^N f_n^{vs,vd} \xi_{0n}^t(\alpha) \right] \quad (31)$$

for  $ka \rightarrow \infty$ , where  $N$  denotes the truncation number of the infinite asymptotic series. In (31), several quantities are defined by

$$\chi_{vs,vd}(\alpha) = B_1 [Q_1(\alpha) \pm \eta_{t2}(\alpha)] + B_2 [\eta_{t1}(\alpha) \pm Q_2(\alpha)], \quad (32)$$

$$C_{s,d} = \pm 1, \quad (33)$$

$$f_n^{vs,vd} = \frac{1}{n!} \left. \frac{d^n \Phi_{+}^{s,d}(\alpha)}{d\alpha^n} \right|_{\alpha=k}, \quad (34)$$

$$\xi_{pn}^t(\alpha) = \frac{e^{2ika}}{\pi} (-1)^p p! \frac{i^{n-p-1/2}}{(2a)^{n-p+1/2}} \cdot \Gamma_{p+1}^t [3/2 + n, -2i(\alpha + k)a], \quad (35)$$

where

$$\eta_{t1,t2}(\alpha) = \frac{\xi_{00}^t(\alpha) - \xi_{00}^t(\pm k \cos \theta_0)}{\alpha \mp k \cos \theta_0}, \quad (36)$$

$$Q_{1,2}(\alpha) = \frac{1}{\alpha \mp k \cos \theta_0} \left[ \frac{1}{K_{+}(\alpha)} - \frac{1}{K_{\pm}(k \cos \theta_0)} \right], \quad (37)$$

$$\Gamma_m^t(u, w) = \int_0^\infty \frac{t^{u-1} e^{-t}}{(t+w)^m} T_{+}[k + it / (2a)] dt. \quad (38)$$

Carrying out some manipulations, we can show the unknowns  $f_n^{vs,vd}$  in (31) are determined by solving the matrix equation

$$f_m^{vs,vd} - C_{s,d} \sum_{n=0}^N A_{mn}^v f_n^{vs,vd} \sim B_m^{vs,vd} \quad (39)$$

for  $m = 0, 1, 2, \dots, N$ , where

$$A_{mn}^v = \sum_{p=0}^m \frac{K_{+}^{(m-p)}(k) \xi_{pn}^t(k)}{p!(m-p)!}, \quad (40)$$

$$B_m^{vs,vd} = \sum_{p=0}^m \frac{K_{+}^{(m-p)}(k) \chi_{vs,vd}^{(p)}(k)}{p!(m-p)!} \quad (41)$$

with

$$K_{+}^{(m-p)}(k) = \left. \frac{d^{m-p} K_{+}(\alpha)}{d\alpha^{m-p}} \right|_{\alpha=k}, \quad (42)$$

$$\chi_{vs,vd}^{(p)}(k) = \left. \frac{d^p \chi_{vs,vd}(\alpha)}{d\alpha^p} \right|_{\alpha=k}. \quad (43)$$

Making use of the above results, we finally arrive at an explicit asymptotic solution to the Wiener-Hopf equation (18) with the result that

$$V_{(+)}(\alpha) \sim K_{\pm}(\alpha) \left[ \mp \frac{B_{1,2}}{K_{\pm}(k \cos \theta_0)(\alpha - k \cos \theta_0)} + B_{2,1} \eta_{t1,t2}(\pm \alpha) + \frac{1}{2} \sum_{n=0}^N (f_n^{vs} \mp f_n^{vd}) \xi_{0n}^t(\pm \alpha) \right] \quad (44)$$

as  $ka \rightarrow \infty$ . A similar procedure may also be applied to (19) for a high-frequency solution, but the details will not be discussed here.

#### 5. Scattered Far Field and Numerical Results

The scattered field in the real space is obtained by taking the inverse Fourier transform of (9) with the result that

$$\phi(\rho, \theta) \sim \hat{\Phi}(-k \cos \theta) k \sin |\theta| (k\rho)^{-1/2} e^{i(k\rho - \pi/4)} \quad (45)$$

as  $k\rho \rightarrow \infty$ . Equation (45) is uniformly valid for arbitrary incidence and observation angles.

We shall now present numerical results on the RCS for the E polarization, and discuss the far field scattering characteristics of the strip in detail. The normalized RCS per unit length is defined by

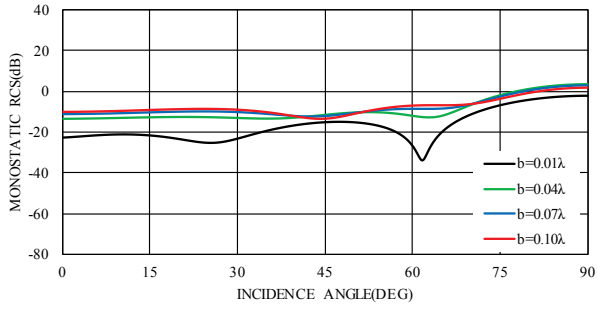
$$\sigma / \lambda = \lim_{\rho \rightarrow \infty} (k\rho |\phi / \phi^i|^2) \quad (46)$$

with  $\lambda$  being the free-space wavelength.

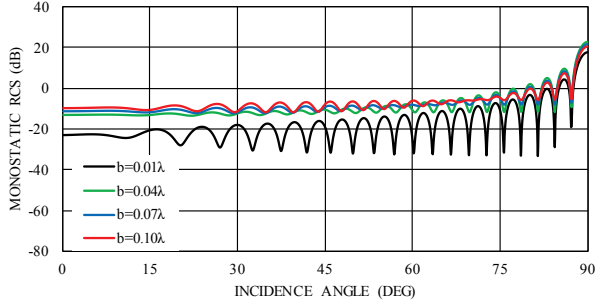
Figure 2 shows the monostatic RCS as a function of incidence angle  $\theta_0$ , where the strip width is  $2a = \lambda, 10\lambda$ , the strip thickness is  $b = 0.01\lambda$ , and the truncation number of the infinite asymptotic series (44) is  $N = 3$ . As an example of existing lossy materials, we have chosen the ferrite [7] with  $\epsilon_r = 12.0 + i0$  and  $\mu_r = 1.4 + i4.5$  in numerical computation. We notice that, for fixed  $2a$ , the RCS level generally becomes larger with an increase of the strip thickness  $b$  except in the neighborhood of  $\theta_0 = 90^\circ$ .

Figure 3 shows the monostatic RCS as a function of incidence angle  $\theta_0$ , where the strip width is  $2a = 10\lambda$ , the strip thickness is  $b = 0.01\lambda$ , and the same material parameters as in Figure 2 have been chosen. Comparing the RCS characteristics for E polarization with those for H polarization [4], we find that the RCS level for H polarization is lower than that for E polarization over the whole range of the incidence angle  $\theta_0$ .

Figure 4 shows comparison with Shapoval's results [8], where the strip dimension is  $2a = 5\lambda$ ,  $b = 0.01\lambda$ , the



(a)  $2a = \lambda$ .



(b)  $2a = 10\lambda$ .

**Figure 2.** Monostatic RCS versus incidence angle  $\theta_0$  for  $\epsilon_r = 12.0 + i0$ ,  $\mu_r = 1$ ,  $N = 3$ .

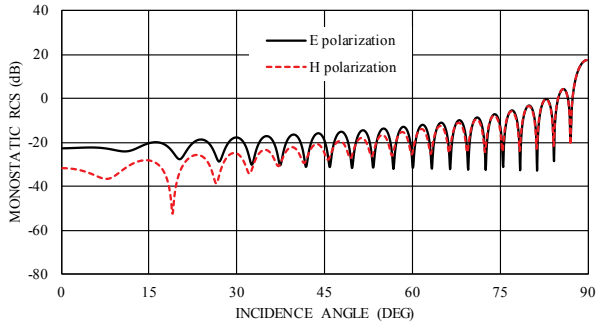


**Figure 3.** Monostatic RCS versus incidence angle  $\theta_0$  for  $2a = 10\lambda$ ,  $b = 0.01\lambda$ ,  $\epsilon_r = 12.0 + i0$ ,  $\mu_r = 1.4 + i4.5$ ,  $N = 3$ .

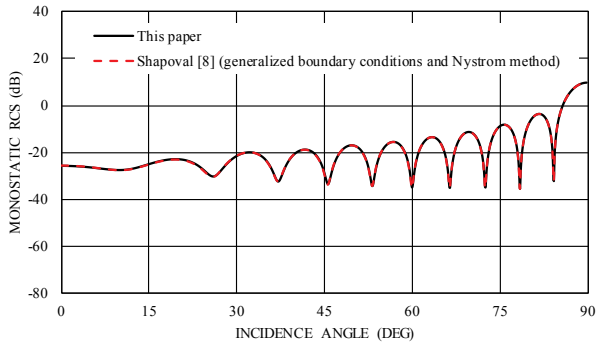


**Figure 4.** Monostatic RCS versus incidence angle  $\theta_0$  for  $\epsilon_r = 3.4 + i0$ ,  $\mu_r = 1$ ,  $2a = 5\lambda$ ,  $b = 0.01\lambda$ ,  $N = 3$ , and its comparison with Shapoval [8].

material parameters are  $\epsilon_r = 3.4 + i0$ ,  $\mu_r = 1$ , and  $N = 3$ . It is seen from the figure that our results agree quite well with Shapoval's results [8].

## 6. Conclusions

In this paper, we have solved the E-polarized plane wave diffraction by a thin material strip using the Wiener-Hopf technique together with approximate boundary conditions. Employing a rigorous asymptotic method, a high-frequency solution for large strip width has been obtained. Illustrative numerical examples on the RCS are presented, and the far field scattering characteristics of the strip have been discussed in detail. Some comparisons with the other existing method have also been provided.

## 7. Acknowledgement

The authors would like to thank Dr. Olga V. Shapoval for providing various numerical results based on generalized boundary conditions and the singular integral equation.

## 8. References

1. J. L. Volakis, "High-frequency scattering by a thin material half plane and strip," *Radio Science*, **23**, 3, 1988, pp.450-462.
2. T. B. A. Senior and J. L. Volakis, *Approximate Boundary Conditions in Electromagnetics*, IEE, London, 1995.
3. O. V. Shapoval, R. Sauleau, and A. I. Nosich, "Scattering and absorption of waves by flat material strips analyzed using generalized boundary conditions and Nystrom-type algorithm," *IEEE Transactions on Antennas and Propagation*, **59**, 9, September 2011, pp.3339-3346.
4. T. Nagasaka and K. Kobayashi, "Wiener-Hopf analysis of the plane wave diffraction by a thin material strip," *IEICE Transactions on Electronics*, **E100-C**, 1, January 2017, pp.11-19.
5. B. Noble, *Methods Based on the Wiener-Hopf Technique for the Solution of Partial Differential Equations*, London, Pergamon, 1958.
6. K. Kobayashi, "Solutions of wave scattering problems for a class of the modified Wiener-Hopf geometries," *IEEJ Transactions on Fundamentals and Materials*, **133**, 5, 2013, pp.233-241.
7. T. Komoni, F. Yasuda and K. Saito, "Development of the demountable damped cavity," *Proceedings of 15th International Conference on RF Superconductivity*, July 2011, pp.172-176.
8. O. V. Shapoval, private communication, September 2016.